MS41 O1

Crystal structure of nanocrystalline manganese oxides

Bruno Lanson[a], Alain Manceau[a], Victor A. Drits[b], [a]*Environmental Geochemistry Group – LGIT, Joseph Fourier University – CNRS, Grenoble, France.* [b]*Geological Institute, Russian Academy of Sciences, Moscow, Russia.*E-mail: bruno.lanson@obs.ujf-grenoble.fr

Keywords: minerals crystal chemistry, disordered structures, environmental sciences

Birnessite is a lamellar manganese oxyhydroxide (phyllomanganate) whose layers are composed of MnO_6 octahedra. Non-stoichiometry arises from the coexistence of heterovalent Mn cations (Mn^{3+}/Mn^{4+}) and/or vacant sites, and is compensated for by the presence of interlayer cations. Despite the low natural concentration of Mn, birnessite is ubiquitous in Nature and plays a pivotal role in geochemical reactions and especially in the fate of pollutants such as organics or heavy metals. Its high reactivity arises from its high surface area, its high cationic exchange capacity, combined with adsorption and redox properties.

In addition to the presence of random stacking faults, the random interstratification of different layer types and the occurrence of well-defined stacking faults are commonly reported in layered minerals, such as phyllomanganates. The high proportion of such defects strongly reduces the efficiency of structure refinement methods, and one effective way to determine the actual structure of defective systems is the calculation of XRD patterns using the mathematical formalism described by Drits & Tchoubar [1].

In particular, this simulation technique allowed showing that layer symmetry depends on the origin of the layer charge deficit. The symmetry of birnessite layers containing vacant octahedra is hexagonal, whereas orthogonal layer symmetry is observed for varieties containing a high proportion (~1/3) of layer Mn^{3+} cations. This distortion arises from the unique azimutal orientation of Mn^{3+} octahedra which are distorted by the Jahn-Teller effect.

In most natural phyllomanganates, and especially in those resulting from biological activity, the abundance of random stacking faults leads to the occurrence of nanocrystalline structures lacking three-dimensional ordering. Even for these turbostratic structures, XRD patterns exhibit noticeable modulations of the 20,11 and 31,02 bands (~2.45 and ~1.42 Å, respectively). These modulations can be used to provide relevant structural information, which includes not only unit-cell parameters but also atomic coordinates and occupancies of the different sites. This information is especially useful to improve our understanding of the interactions between natural phyllomanganates and environmentally important heavy metals.

The usefulness of this approach will be illustrated with various synthetic and natural birnessite samples.

[1] Drits V.A. & Tchoubar C. (1990): X-ray diffraction by disordered lamellar structures. Springer Verlag, Berlin, 371 p.

MS41 O2

Te-Te interaction in minerals and inorganic compounds.

Herta Effenberger *Institut für Mineralogie und Kristallographie, Universiät Wien, Vienna, Austria.* E-mail: herta.silvia.effenberger@univie.ac.at

Keywords: tellurides, Te—Te interaction, charge balance

Compounds with tellurium atoms coordinating cations are frequently found in nature; due to the interest in their catalytical properties and semiconducting behaviour they were synthesized as well. In most of these cases the Te atoms have a formal charge of 2-. However, in some cases the Te atoms are also linked to each other and form covalently bonded pairs of chalcogen atoms. The Te—Te bond distances are similar to that of native tellurium (the infinite helices have Te—Te bond distances of 2.835(2) Å and Te—Te—Te bond angles of 96.3(2)°). Common are $M\mathrm{Te}_2$ compounds crystallizing in the pyrite or marcasite type. They have dumbbells Te_2 in analogy to S_2 or Se_2. However, tellurides have a greater propensity than selenides or sulfides to exhibit interactions intermediate between a single Te—Te bond and a $Te^{2+}\cdots Te^{2+}$ interaction. Te atoms form also Te_3 groups, which were found *e.g.*, in AgTe (empressite), $Rb_4Hg_5(Te_3)_2(Te_2)_2Te_3$, $K_2Cu_2(Te_3)(Te_2)$, or $K_4[Hf_3(Te_3)(Te_2)_7]$. — Buckhornite, $[(Pb_2Bi)S_3](AuTe_2)$ and nagyagite, $[(Pb_3(Pb,Sb)_3S_6](Au,Te)_3$ are member of a homologue series. In buckhornite two (Pb,Bi)S sheets form one slice of the SnS archetype whereas in nagyagite four (Pb,Sb)S layers form the corresponding slice with a thickness of two SnS-archetype slabs. These layers are separated in both compounds by Au—Te *mono*-layers. In buckhornite an ordering of the Au and Te atoms on two different crystallographic sites with site symmetries *mm*2 and *m*, respectively, was observed. The symmetry elements are perpendicular to the gold-tellurium layers. The Au(III) atoms are [4] coordinated with Au—Te bond distances of 2.71 Å. The coordination figure is practically planar. The $AuTe_4$ configurations in buckhornite share each two *trans*-arranged Te—Te edges to form ribbons with the formula $AuTe_2$. The Te—Te distances are 3.52 Å and 4.11 Å for the shared and unshared edges within the $AuTe_4$ configuration. The Te—Te distances between the $AuTe_2$ ribbons are 3.34 Å and indicate weak Te—Te contacts. It is remarkable that they are shorter than the Te—Te edges within the $AuTe_4$ configuration. In the average nagyagite structure Te and Au paradoxically have to be assigned to one atomic position with site symmetry *m*. From this occupation results a formal square-planar (Te,Au) net. In nagyagite Au:Te varies on a wide scale (it scatters in most analyses roughly from 1:2 to 1:3), in buckhornite the ratio Au:Te is close to 1:2. In nagyagite the average (Te,Au)—(Te,Au) distance of 2.97 Å features statistically a mean value of Au—Te and Te—Te. The ratio of covalent Te—Te bonds and unbounded Te···Te contacts serve for local charge balance in accordance with the PB.Sb ratio in the SnS archetype layer. — In this context the pseudo-binary $(Au,Ag)Te_2$ minerals calaverite, krennerite and sylvanite are worth to be mentioned. The average structures correspond roughly with a distorted CdI_2-structure type. Valence fluctuations are the driving force for the incommensurately modulated crystal structure of calaverite ($AuTe_2$). Krennerite ($Au_{0.8}Ag_{0.2}Te_2$) can be considered as twin interface modulated long period superstructure of calaverite.

MS41 O3

Correlation between optical constants and crystal chemical parameters of ZrW_2O_8

Reinhard X. Fischer[a], Olaf Medenbach[b], Robert D. Shannon[c] [a]*Fachbereich Geowissenschaften, Universität Bremen, Germany.* [b]*Institut fürMineralogie, Universität Bochum, Germany.* [c]*Geological Sciences/ CIRES, University of Colorado, Boulder, USA*. E-mail: rfischer@uni-bremen.de

Keywords: optical constants; polarizabilities; ZrW_2O_8

ZrW_2O_8 is unusual because of its negative thermal expansion coefficient over the range 0.3 to 1050 K [1]. The refractive index, n_D, of ZrW_2O_8 was reported to be 1.669 [1], but this value appears to be rather low for a tungstate which usually have values in the range between 1.84 and 2.27. The refractive index of ZrW_2O_8 was redetermined at wavelengths between 435.8 nm to 643.8 nm yielding the n_D value at $\lambda = 589.3$ nm. The corresponding n_∞ was extrapolated from the dispersion curve for $\lambda = \infty$ using two forms of the one-term Sellmeier equation: (1) $1/(n^2-1) = -A/\lambda^2 + B$ where A, the slope of the plot of $(n^2 - 1)^{-1}$ vs. λ^{-2} in units of 10^{-16} m^2 gives a measure of dispersion and B, the intercept of the plot at $\lambda = \infty$, gives $n_\infty = (1 + 1/B)^{1/2}$, and (2) $n^2-1 = E_d E_o /(E_o^2 - (\hbar\omega)^2)$, where $\hbar\omega$ = the photon energy, E_o = the average single oscillator (Sellmeier) energy gap and E_d = the average oscillator strength, which measures the strength of interband optical transitions. Refractive indices, n_D and dispersion values, A, were, respectively, 1.8794 and 114 x 10^{-16} m^2. The high dispersion is attributed to the low value of E_o = 7.7 eV. The total polarizabilities, α_{total}, were calculated from n_∞ and the Lorenz-Lorentz equation. The unusually large difference between the observed polarizability of 20.087 Å^3 and the calculated total polarizability α_T of 17.63 Å^3 (Δ = +12.2%) [2] is attributed to large M-O-M' angles resulting in a high degree of W *5d* – O *2p* and Zr *nd* – O *2p* hybridization, especially in the case of terminal oxygen atoms (Fig. 1) present in ZrW_2O_8. The relationship between atomic displacement factors B(O) of oxygen normalized to B(W) is discussed.

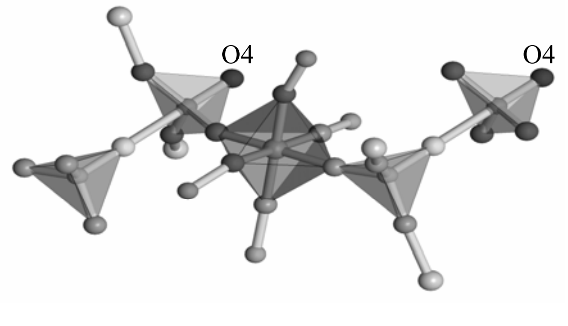

Fig. 1: Projection of the crystal structure of ZrW_2O_8 [1] with terminal oxygen atoms O4.

[1] Evans, J.S.O.; Mary, T.A.; Vogt, T.; Subramanian, M.A.; Sleight, A.W.; *Chem. Mater.*, 1996, 8, 2809.

[2] Shannon, R.D.; Fischer, R.X. *Phys. Rev.* 2006, B73, 235111.

MS41 O4

Simulating extended structures: a powerful crystallographic tool when interpreting X-ray absorption spectroscopy data

Maria-Ondina Figueiredo, *Dept. of Materials Science, New University of Lisbon, 2829-516 Caparica & INETI/IGM, Portugal.*
E-mail: ondina.figueiredo@ineti.pt

Keywords: XAFS, local order, crystal structure prediction.

Within the actual development of Materials Science, combining the crystal structure of selected model compounds with local atomic arrangement inferred by X-ray absorption spectroscopy is fundamental for a successful interpretation of either XANES (near-edge features) or EXAFS data. Currently used analytical (mathematical and physical) methodologies for theoretical data fitting have enhanced the need for an increased capability of idealizing and simulating appropriate atomic geometries. With no doubt, theoretical crystallography plays a unique role in predicting local environments suitable to match the structural information provided by an element selective approach like X-ray absorption spectroscopy with convoluted results obtained through a bulk technique, namely, X-ray diffraction [1].

Two examples are described to illustrate such novel role of Crystallography. One is the handling of cubic tetrahedrites, [c P 58 : $P\bar{4}3n$ (6d) (6c)**.**$(12f)^x$**.**$(8e)^x$**.**$(24i)^{xyz}$**.**(2a)], with ideal formula $M_{12}^{t}\ M_{12}^{tr}\ (M^{3+})_8^{\pi}\ \{\ [S_{24}^{t}].\ [S_2^{t}]\ \}^{<c>}$ (M = Cu, Ag, Zn, Fe, Cd, Pb; M^{3+} refers to Sb, As, Bi). In this structural formulation, $\underline{t}$ stands for tetrahedral, $\underline{tr}$ for triangular, $\underline{\pi}$ for pyramidal coordination and $\underline{c}$ denotes the cubic closest packing of sulphur anions where four vacant sites out of sixteen packing positions are replaced by one sole S-atom [2], towards a progressive approximation to the ideal tetrahedral array found in sphalerite structure-type, $Zn^t\ [S^t\ ]^c$, [c F 8 : $F\bar{4}3m$ (4a)**.**(4c)]. This approach is now being applied to interpret S *K*-edge XANES spectra and, desirably, the electronic structure of sulphur in this mineral group.

Another example concerns the partial and disordered of substitution of potassium by lead in the crystal structure of jarosite [3], $K^{ic}\ Fe^{o}_3\ (S^{t}O_4)_2\ (OH)_{6-x}\ (H_2O)_x$, where $\underline{ic}$ stands for pseudo-icosahedral and $\underline{o}$ for octahedral coordination. Kipping the trigonal space group $R\bar{3}m$ and allowing for the replacement of potassium invariant position (3a) with site symmetry [$\bar{3}m$] by the equipoint (18h) with free parameters $\underline{x},\underline{z}$ and lower site symmetry [. *m*], it becomes possible to generate a local environment particularly suitable to accommodate the lone $6s^2$ electron-pair of Pb^{2+} ions.

A detailed description is presented of these two type-cases illustrating the fruitful interplay between XAFS and Crystallography.

[1] Figueiredo, M.O., *X-ray Absorption Fine Structure – XAFS13*, edt. B. Hedman & P. Pianetta, 2007, AIP Conf. Proceedings 882, 205.

[2] Ferreira, J.A.; Figueiredo, M.O. *Mitt. Österr. Mineralog. Gesellschaft* 2004, 149, 30.

[3] Szymanski, J.T., *Canad. Miner.,* 1985, 23, 659.